Structure of DNA–Cationic Surfactant Complexes at Hydrophobically Modified and Hydrophilic Silica Surfaces as Revealed by Neutron Reflectometry

ARTICLE *in* LANGMUIR · AUGUST 2011

Impact Factor: 4.46 · DOI: 10.1021/la202087u · Source: PubMed

4 AUTHORS, INCLUDING:

Marité Cárdenas
Malmö University
54 PUBLICATIONS **793** CITATIONS

SEE PROFILE

Langmuir

ARTICLE

pubs.acs.org/Langmuir

Structure of DNA−Cationic Surfactant Complexes at Hydrophobically Modified and Hydrophilic Silica Surfaces as Revealed by Neutron Reflectometry

Marité Cárdenas,*[,†] Hanna Wacklin,[‡,§] Richard A. Campbell,[‡,∥] and Tommy Nylander[∥]

[†]Nanoscience Center and Institute of Chemistry, Copenhagen University, Universitetsparken 5, DK-2100 Copenhagen E, Denmark

[‡]Institut Laue-Langevin, 6 rue Jules Horowitz, BP 156, 38042 Grenoble, France

[§]European Spallation Source ESS AB, P.O. Box 176, 221 00 Lund, Sweden

[∥]Physical Chemistry, Department of Chemistry, Lund University, P.O. Box 124, SE-22100 Lund, Sweden

ABSTRACT: In this article, we discuss the structure and composition of mixed DNA−cationic surfactant adsorption layers on both hydrophobic and hydrophilic solid surfaces. We have focused on the effects of the bulk concentrations, the surfactant chain length, and the type of solid surface on the interfacial layer structure (the location, coverage, and conformation of the DNA and surfactant molecules). Neutron reflectometry is the technique of choice for revealing the surface layer structure by means of selective deuteration. We start by studying the interfacial complexation of DNA with dodecyltrimethylammonium bromide (DTAB) and hexadecyltrimethylammonium bromide (CTAB) on hydrophobic surfaces, where we show that DNA molecules are located on top of a self-assembled surfactant monolayer, with the thickness of the DNA layer and the surfactant−DNA ratio determined by the surface coverage of the underlying cationic layer. The surface coverages of surfactant and DNA are determined by the bulk concentration of the surfactant relative to its critical micelle concentration (cmc). The structure of the interfacial layer is not affected by the choice of cationic surfactant studied. However, to obtain similar interfacial structures, a higher concentration in relation to its cmc is required for the more soluble DTAB surfactant with a shorter alkyl chain than for CTAB. Our results suggest that the DNA molecules will spontaneously form a relatively dense, thin layer on top of a surfactant monolayer (hydrophobic surface) or a layer of admicelles (hydrophilic surface) as long as the surface concentration of surfactant is great enough to ensure a high interfacial charge density. These findings have implications for bioanalytical and nanotechnology applications, which require the deposition of DNA layers with well-controlled structure and composition.

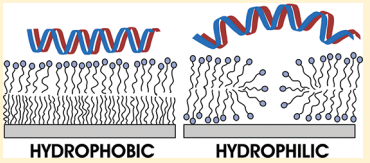

INTRODUCTION

Complexes of DNA with cationic species are important in living systems as well as in a range of applications, which has promoted a large variety of studies in the last decades. DNA separation and purification methods were developed as early as 1967 on the basis of the characteristic phase separation that occurs in the presence of cationic surfactants.[1,2] The potential of using DNA−cationic surfactant (or lipid) systems (lipoplexes) as nonviral vectors for gene delivery has been recognized, and the number of studies of such systems has therefore increased during recent years.[3,4] The stability of lipoplexes at biological interfaces is crucial given that gene delivery particles must circulate in the bloodstream for several hours,[4] where they will encounter different types of interfaces that they are likely to interact with, which can influence the uptake of DNA at the target. Hence, determining the interfacial behavior of lipoplexes is a key parameter in designing efficient gene delivery systems. In mixed solutions of oppositely charged polymers and surfactants, associative phase separation as a consequence of the attractive interaction between the surfactant and the polymer is a well-known phenomenon,[5,6] and many of the features from such system are also observed for the DNA/cationic surfactant systems. In the bulk, surfactant addition to a DNA solution will therefore lead to an initial complexation on the single-molecule scale, at a so-called critical association concentration (cac) that is below the cmc of the surfactant. The cooperativity has been demonstrated for a range of DNA condensing agents such as multivalent ions, cationic lipids, and surfactants, and the consequence is the collapse of the DNA coil on the single-chain level as a discrete all-or-none type of transition to a globule.[7−10] If the surfactant concentration is further increased above this point, then the complexes formed by individual DNA molecules aggregate and precipitate out of the solution. Such phase separation is believed to occur via a compensation of the electrical charges of the DNA molecule, which decreases the aqueous solubility of the complexes. The structure of the precipitated phase resembles the liquid-crystalline structures formed by the surfactant (complexing agent) and includes lamellar, hexagonal, cubic, and other types of mesophases.[11−15] The formation of DNA and cationic lipid/surfactant complexes at interfaces differs from the corresponding process in the bulk solution in that complex formation occurs over a different

Received: November 28, 2010
Revised: August 13, 2011
Published: August 29, 2011

dx.doi.org/10.1021/la202087u | *Langmuir* 2011, 27, 12506–12514

concentration regime.[16,17] This implies that for given bulk concentrations of DNA and surfactant, the interfacial complexes may have a different composition, structure, and morphology as compared to those of the bulk complexes,[8,12−14] especially given the confinement of an interface and the fact that the local concentration of surfactant molecules in the adsorbed layer is higher than in the bulk.[18] In fact, the apparent cac for DNA−surfactant complexes at an interface (i.e., the bulk concentration at which significant adsorption is observed on a surface), occurs at a lower concentration than the bulk cac because the local concentration of surfactant is enhanced at the interface. The structure of the interfacial complexes might also be different from the structure of the bulk complexes.[8,12−14] Indeed, the structure of DNA−surfactant/lipid complexes at the air−water interface has been investigated using neutron reflection among other techniques.[19,20] The interfacial layer was found to be made of a surface monolayer of surfactants at the air−water interface, below which a monolayer of DNA is attached. For further increases in the surfactant concentration, an additional layer of surfactant micelles was detected below the DNA layer.[19] However, for cationic surfactants, such as alkyltrimethyl ammonium bromide derivates, the structures of the bulk precipitates resemble reversed hexagonal or cubic phases, and a lamellar phase was found for phospholipids. Interestingly, at the air−water interface the type of surfactant seems to have a minor impact on the organization within the mixed adsorbed film.[19,20]

We have previously studied the interaction of DNA and cationic surfactants in the bulk as well as coadsorption of the resulting complexes on hydrophobic and hydrophilic silica surfaces using a variety of techniques such as null ellipsometry, surface force measurements, dynamic light scattering, and neutron scattering.[18,21−25] The motivation for this work was to increase our understanding of DNA compaction at surfaces in the presence of cationic surfactants. In this context, we define surface compaction as the process where strong attractive electrostatic interactions confine the DNA strand close and parallel to the interface. The compaction of single DNA molecules with cationic surfactants in the bulk, without the confinement of the interface, tends to give spherical aggregates of a single DNA molecule at low surfactant concentrations, where the hydrodynamic radius of the complex is significantly smaller than the hydrodynamic radius of pure DNA.[24]

In this study, we have investigated the effect of two homologous cationic surfactants with different acyl chain lengths, namely, hexadecyltrimethylammonium bromide (CTAB) and dodecyltrimethylammonium bromide (DTAB) at concentrations 15 and 150 times below their critical micelle concentrations (cmc) in 10 mM NaBr, which are 0.15 and 11 mM,[26] respectively. We study complexes between soluble single DNA molecules condensed into globules by the cationic surfactant that are stable in solution, and thus are likely to carry a partial negative charge.[14,18,21,27] For the highest surfactant concentration (15 times lower than the cmc) used in this study, we note that in the bulk solution single noncompacted DNA molecules coexist with the monomeric CTAB molecules[21,28] and DNA/surfactant globules are present for DTAB.

Our previous results from ellipsometry measurements show that the adsorption of DNA occurs on hydrophobic surfaces and the addition of cationic surfactants induces layer reorganization from a diffuse, thick DNA layer to a compact, dense layer of DNA and surfactants. The concentration required to compact DNA on hydrophobic surfaces is far below the cmc of the surfactant and also much below the concentration required for bulk compaction: in the bulk, 0.030 mM CTAB is required to observe globules at a DNA concentration of 0.02 mg/mL DNA (0.061 mM negative charges) in 10 mM NaBr, that is, at a 0.5 cationic surfactant per negative DNA charge, as determined by fluorescence microscopy.[21,28] Under identical conditions on hydrophobic surfaces, DNA compaction was observed at CTAB concentrations of as low as 0.001 mM, that is, 1 cationic surfactant per 60 negative DNA charges in the bulk solution.[12] In the absence of DNA, some adsorption occurs for CTAB under identical conditions,[12,23] although the adsorbed layer is far from being saturated (<0.5 mg/m^2 compared to the plateau value of 1.76 mg/m^2). If the bulk surfactant concentration is increased in the presence of DNA while remaining below the phase separation border, it does not lead to any significant increase in the adsorbed amount or changes in thickness.[23] Thus, DNA molecules seems to be attached to the oppositely charged surface, and the steady-state adsorption plateau value is reached at a significantly lower surfactant concentration than what is required for plateau adsorption of the surfactant alone.

On hydrophilic surfaces, adsorption occurs only very close to the phase-separation boundary: 0.06 mg/mL DNA (0.182 mM negative charges) requires ∼0.6 mM DTAB for adsorption to occur. Thus, there are about 3 times as many cationic surfactants as negative charges from the DNA in the bulk solution. Further increases in the bulk surfactant concentration to 0.7 mM leads only to additional adsorbed mass while the mean layer thickness remains constant.[21] In all of our DNA compaction studies at the solid−liquid interface,[29] we have systematically observed no adsorption from DNA−CTAB solution complexes prior to phase separation when high-molecular-weight DNA (salmon sperm) was used.[21,29] If we instead used low-molecular-weight DNA (crude herring sperm DNA),[29] then we did observe significant adsorption before phase separation using CTAB. Later analyses of this low-molecular-weight DNA sample revealed that it was highly polydisperse and contained a significant amount of protein (unpublished data). Our studies on short DNA samples thereafter are based on higher-quality samples than crude herring sperm DNA. This is the reason that we used DTAB for the present study of complex formation at the hydrophilic surface.

The adsorbed amount and average layer thicknesses measured with ellipsometry under the conditions chosen for DNA−cationic surfactant complexes on hydrophobic and hydrophilic silica surfaces show no striking differences in terms of the plateau values of the adsorbed amount at high surfactant concentration, even though the surface properties and the chain lengths of the cationic surfactants differ. The question arises as to how the composition and the organization of the DNA−surfactant is affected by the changes in solution composition and surfaces properties. The lack of such structural information available from ellipsometry prompted the present investigation with neutron reflectivity, which allowed us to obtain more detailed structural information as well as the composition of the adsorbed layer. In this article, we describe the structure, coverage, and composition of DNA and cationic surfactant layers at the surface of hydrophobically modified and hydrophilic silica surfaces measured by neutron reflectometry (NR). NR allows the identification of the surface layer structure by means of hydrogen/deuterium substitution with different isotopic contrasts of the surfactant and the solvent.[30,31] We present here a thorough characterization of the structure of DNA/cationic surfactants at interfaces, first of a

Table 1. Summary of Experimental Variables in the Four Systems under Investigation

system	surface	surfactant	DNA conc (mg/mL/ mM negative charges)	surfactant conc (mM)	surfactant conc/cmc
DTAB-cmc/15-HPHOB reference system	hydrophobic	DTAB	0.06/0.182	0.7	1/15
DTAB-cmc/150-HPHOB effect of bulk conc	hydrophobic	DTAB	0.02/0.061	0.07	1/150
CTAB-cmc/150-HPHOB effect of surfactant	hydrophobic	CTAB	0.02/0.061	0.001	1/150
DTAB-cmc/15-HPHIL effect of surface	hydrophilic	DTAB	0.06/0.182	0.7	1/15

reference system comprising DNA with DTAB (at cmc/15) on hydrophobic surfaces followed by the effect of lowering the bulk surfactant concentration by a factor of 10, thus increasing the surfactant chain length and changing the type of solid substrate. A good understanding of the physical variables that influence the adsorption process and resulting interfacial structures is crucial to determining the stability of DNA lipoplexes in the biological environment with a view to potential applications in gene delivery.

EXPERIMENTAL SECTION

Materials. Salmon sperm DNA was purchased from Gibco, BRL, and was used as received. As stated by the manufacturer, this DNA is double-stranded and 2000 ± 500 base pairs (bp) long, as determined by 1% TAE agarose gel analysis, and is free from DNase and RNase. Hexadecyltrimethylammonium bromide (CTAB) and dodecyltrimethylammonium bromide (DTAB) from Merck (pa quality) and sodium bromide from Aldrich (extra-pure quality) were used as received. Dimethyloctylchlorosilane (Me_2−OdCS) was obtained from Sigma-Aldrich (97% purity) and was used as received. Chain-deuterated surfactants were a kind gift of Dr. Robert K. Thomas, University of Oxford, United Kingdom. Water purified by a Milli-Q system (Millipore Corporation, Bedford, MA) and D_2O (Euriso-top, C.E. Saclay, France) were used in all measurements. All DNA and surfactant solutions were prepared in a 10 mM NaBr solution.

Methods. In neutron reflectometry (NR), the specular reflectivity from a flat surface is measured as a function of momentum transfer (Q)

$$Q = \frac{4\pi \sin \theta}{\lambda} \quad (1)$$

where θ is the angle of incidence and λ is the wavelength.[32] The neutron reflectivity profiles are presented as the intensity ratio of the specular reflection with respect to the incident neutron beam, corrected for background scattering. A further description of the theory and applicability of NR can be found, for example, in the review by Thomas.[33] The experiments were performed on the FIGARO[34] and D17[35] reflectometers at the Institut Laue-Langevin (ILL), Grenoble, France.[35] The instruments were operated in time-of-flight mode using neutron wavelengths of 4−24 Å on FIGARO (systems A and B; constant $d\lambda/\lambda$ of 5.6%) and 2−20 Å on D17 (systems C and D; variable $d\lambda/\lambda$ of ∼5%). (See Table 1 for a summary of the systems studied.)

A liquid flow cell of ∼5 mL was used, where the reflecting surface of the solid substrate was vertically oriented on D17 (see Vandoolaeghe et al. for further details[36]) and horizontally oriented on FIGARO. The aluminum casing of the cells was thermostatted at 25.0 ± 0.1 °C, and the internal liquid trough, made of Teflon, was equipped with a magnetic stirrer. Sample injections were accomplished by flowing through at least 20 mL (i.e., 4 times the cell volume) to ensure the efficient exchange of the bulk solution.

Surface Preparation. The NR substrates used were single crystals of silicon (Si) with dimensions of 5 cm × 5 cm × 1 cm cut along the (111) face and commercially polished (Siltronix, France). The hydrophilic surfaces were cleaned in dilute piranha solution consisting of water, sulfuric acid (98%), and hydrogen peroxide (27.5% solution in water) in a 5:4:1 volume ratio at 80 °C for 15 min, which provided effective cleaning yet preserved the low roughness of the native oxide layer. To prepare the hydrophobic silica surfaces, the crystals were dried under vacuum and treated in a plasma cleaner (Harrick Scientific Corporation, model PDC-3XG) in low-pressure air (0.02 mbar) for 5 min. Then they were placed in a vessel containing 2 mL of liquid Me_2−OdCS and were subjected to silane vapor at reduced pressure for 24 h at room temperature. The hydrophobized silicon crystals were then rinsed in ethanol and tetrahydrofuran. Before use, they were thoroughly rinsed in ethanol and water. To avoid any air or depletion layer[37] at the hydrophobic surface, ethanol was pumped through the flow cells before the aqueous solution was used.

Approach. The scope of the present work was to study the interaction of DNA with cationic surfactants on solid substrates and to elucidate the interfacial structure with respect to important variables such as the bulk concentration, the surfactant chain length, and the type of surface. Four systems were studied, the details of which are summarized in Table 1. First, we defined a reference system of 0.06 mg/mL DNA (0.182 mM negative charges) with 0.7 mM DTAB on a hydrophobic surface (DTAB-cmc/15-HPHOB). The primary requirement in this system was to produce favorable adsorption conditions and avoid uncontrolled aggregation due to phase separation in the bulk (which starts at 0.8 mM DTAB for this DNA concentration). The first variable to be assessed was the effect of the bulk concentration (DTAB-cmc/150-HPHOB) where the amount of DTAB was reduced by 1 order of magnitude (0.070 mM) and the amount of DNA was reduced by a factor of 3 (0.061 mM negative charges). The DNA concentration was kept the same in the next system in which a longer acyl chain surfactant was used (CTAB-cmc/150-HPHOB) at 0.001 mM (the same concentration ratio with respect to the cmc as for DTAB-cmc/150-HPHOB) because higher bulk surfactant concentrations would be in the phase separation region. For the DNA−CTAB system, the phase separation region with 0.02 mg/mL DNA (0.061 mM negative charges) starts at just 0.007 mM CTAB.[28] Increasing the bulk CTAB concentration to above $^1/_{150}$ cmc does not change the net adsorbed amount or layer thickness,[21,28] and thus these conditions should be preferable given the motivation of potential gene delivery applications as well as the well-known toxicity of cationic surfactants. The final variable under investigation was the type of surface, changing from hydrophobic to hydrophilic silica (DTAB-cmc/15-HPHIL). Here, we return to precisely the same bulk conditions as in our reference DTAB-cmc/15-HPHOB because on hydrophilic surfaces DNA adsorbs only in the presence of DTAB (and not CTAB) below the concentration regime where bulk phase separation starts.[21] This is due to the shorter alkyl chain of DTAB (4 carbon atoms shorter than that of CTAB) that makes its cmc 2 orders of magnitude higher than that of CTAB under the conditions used in this work.

Methodology. NR measurements were carried out in several isotopic contrasts of the solvent to allow for the simultaneous fitting of the data to determine the amounts of surfactant and DNA in the layers. Before the exposure of the surfaces to DNA and cationic surfactants, which was carried out by the injection of premixed solutions, the reflectivity profiles of the native oxide layer and (where applicable) the silane layer were measured. The surfactants and DNA were mixed

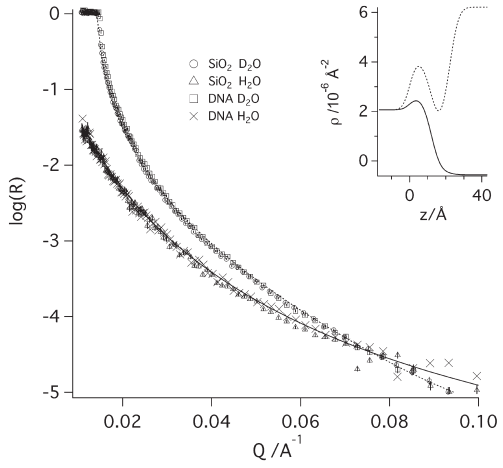

Figure 1. Representative neutron reflectivity profiles for a hydrophobic surface before and after exposure to 0.02 mg/mL DNA. The lines show best fits to the clean hydrophobic surface. The inset gives the scattering length density profiles obtained for the best fits given in the main panel. There was a natural SiO_2 layer of 12 ± 2 Å with 15 ± 5% solvent content and a hydrophobic layer of 10 ± 1 Å with 25 ± 5% solvent content, with a typical roughness of 3 Å.

Table 2. Scattering Length Densities for the Substrate, Solvents, and Compounds Used in This Study

material	ρ (10^{-6} Å^{-2})	V_m (Å^3)
Si	2.07	
SiO_2	3.41	
Me_2−OdCS	−0.40	
D_2O/H_2O	6.35/−0.56	
hCTAB	−0.37	524[a]
dCTAB	5.61	524[a]
hDTAB	−0.31	413 [a]
dDTAB	5.51	413[a]
DNA (D_2O/H_2O)	4.05/3.40[49]	1178[b]

[a] Calculated from the densities given in ref 50. [b] Calculated from the area of a cylinder in which the radius is given by half the diameter of B-DNA and the length is given by the pitch of B-DNA, which corresponds to 34 Å and 10 base pairs.[42]

immediately before sample injection by pouring together equal volumes of twice the intended concentrations of each species. NR profiles of interfacial layers with the same chemical structure and composition but with different isotopic compositions of either the surfactant and/or the solvent were measured sequentially. Either a chain-deuterated surfactant or a fully hydrogenated surfactant was used in three different solution contrasts: D_2O, H_2O, and cmSi (a mixture of 38 v/v% D_2O and 62 v/v% H_2O, contrast matched to bulk silicon). In this way, we could selectively record reflectivity profiles most sensitive to the surfactant (h-surfactant in D_2O and d-surfactant in cmSi), the DNA (d-surfactant in D_2O), or both (d-surfactant in H_2O). As in previous ellipsometry experiments, final measurements of the interfacial layer after several solution exchanges demonstrated that the layers had not undergone changes in structure or chemical composition as a result of the various solution exchanges.

The pre-exposure of a hydrophobized silica surface to DNA (in the absence of surfactant) induced only minimal DNA adsorption corresponding to 0.003 negative charge/Å^2, as measured with null

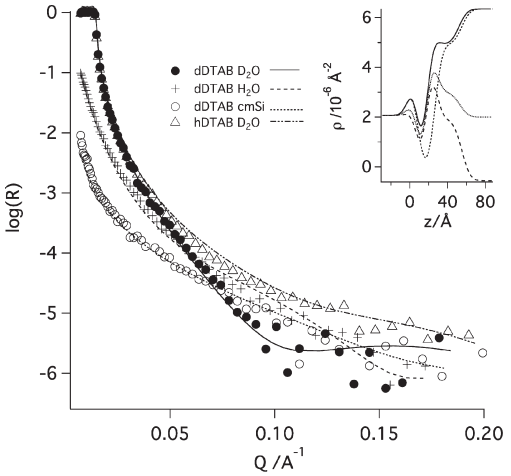

Figure 2. DTAB-cmc/15-HPHOB or the reference system. Neutron reflectivity profiles of 0.182 mM negative charges of DNA (0.06 mg/mL) and 0.7 mM DTAB on a hydrophobically modified silicon surface. Four different isotopic contrasts were used where the symbols and lines correspond to data and fits, respectively: a fully deuterated surfactant in D_2O (●), H_2O (+), and cmSi (○) and a fully hydrogenated surfactant in D_2O (△). The inset gives the scattering length density profiles obtained for the best fits (—) given in the main panel.

ellipsometry.[18] We confirmed this with NR: Figure 1 shows that NR profiles recorded in two different solvent contrasts cannot be distinguished from those of the same surface before exposure to DNA. After this pre-exposure and extensive rinsing with buffer, DNA−CTAB mixtures were introduced onto the same surface in all experiments with CTAB-cmc/150-HPHOB.

Data Analysis. The neutron scattering from different isotopes of the same element can differ significantly as a neutron interacts with the nucleus of an atom. This allows for contrast variation by isotopic substitution, particularly by deuterium substitution for hydrogen, in which there is a large difference in their coherent scattering. The scattering length density (ρ) of a material is expressed as

$$\rho = \sum n_i b_i \tag{2}$$

where n is the number of nuclei in a given volume and b is their coherent scattering length.[38] Table 2 shows the scattering length densities for the substrate, solvents, and chemical compounds used in this study. All neutron reflectivity profiles obtained in this study were analyzed by fitting simulated reflectivity profiles to the experimental data in Motofit,[39] which uses the Abeles optical matrix method[40] to calculate the reflectivity of thin layers and enables the global fitting of data sets of different isotopic compositions. The fitting parameters used for each layer were the thickness (d), the interfacial roughness (δ), the scattering length density ρ of the material, and the solvent volume fraction (ϕ). The adsorbed amount, Γ, was calculated from the fits using the following equation:

$$\Gamma = \frac{(1-\phi)*d*\mathrm{MW}}{V_m*N_{AV}} \tag{3}$$

where MW and V_m are the molecular weight and volume of the component in each layer, respectively, and N_{AV} is Avogadro's number.

A two-layer interfacial model (SiO_2−Me_2OdCS) was used to fit neutron reflectivity profiles of the bare hydrophobic surface, and a one-layer interfacial model (SiO_2) was used for the bare hydrophilic surface. In each case, the data were fitted simultaneously to three isotopic solution contrasts: D_2O, H_2O, and cmSi. A four-layer interfacial model (SiO_2−Me_2OdCS−surfactant−DNA) was used to fit the reflectivity

profiles of the mixed adsorption layer on the hydrophobic surface, and a three-layer interfacial model (SiO_2−surfactant−DNA) was used for the adsorption layer on the hydrophilic surface.

RESULTS AND DISCUSSION

DTAB−DNA on a Hydrophobic Surface at $^1/_{15}$th of the cmc (DTAB-cmc/15-HPHOB). We started our structural characterization of DNA/surfactant adsorption layers at surfaces with a reference system: 0.06 mg/mL DNA (0.182 mM negative charges) with 0.7 mM DTAB on hydrophobic surfaces. Neutron reflectivity profiles of DNA−DTAB mixtures on hydrophobic surfaces under these conditions are shown in Figure 2 along with the corresponding best fits to the measured data. Table 3 gives the parameters used in the fits. We could imagine three different structures for the mixed DNA−surfactant layer on a hydrophobic substrate. In model 1, DNA is directly adsorbed onto the surface and the cationic surfactants form a bilayer or micelles on top of the DNA layer. In model 2, a DTAB monolayer is instead in direct contact with the hydrophobic substrate and DNA is located on top of this monolayer. In model 3, there is an additional layer of DTAB micelles/bilayer on top of the DNA facing the bulk solution. Simulated reflectivity profiles for the most sensitive contrast for the overall mixed layer, h-DTAB in D_2O, for appropriate examples of these three models are shown in Figure 3, along with the corresponding measured data for the same contrast. The simulation that clearly fits the data best corresponds to model 2, in which DNA molecules are located on top of a monolayer of DTAB without any DTAB adsorbed above it (to which the sensitivity of the measurement is ±5 vol/vol%). Excellent fits using model 2 were obtained for all four contrasts shown in Figure 2, further validating the result, which is schematically represented in Figure 8.

At the air/water interface, which can also be considered to be a hydrophobic surface, DTAB forms a monolayer about 15 Å thick with an area per molecule of 48 Å when adsorbed from solutions close to the cmc.[41] However, in the present study the homogeneous box model indicates a DTAB layer that is only 9 ± 1 Å thick and contains 9% solvent by volume. Both interfaces between the surfactant monolayer and Me_2OdCS/DNA layers are 6 Å rough, which means that the fitted box thickness for the surfactant monolayer does not describe the true layer structure adequately but implies that there is significant intercalation or interdigitation between the surfactant and both Me_2OdCS and the DNA layer. Thus, the monolayer coverage derived from the box thickness alone cannot be used to calculate the true surface coverage or area per molecule, and the values in Table 3 are only guidelines to show the relative thickness/roughness values and the fitting uncertainties. The diameter of the B-DNA helix is 21 Å,[42] in relatively good agreement with the fitted layer thickness of 26 ± 2 Å, which means that the electrostatic interaction between DNA and the cationic surfactant layer is strong enough to compensate for the loss of conformational entropy of the DNA and results in a nearly flat orientation parallel to the monolayer of DTAB. The DNA layer (which includes 38 ± 5 v/v % solvent) has a thickness that is slightly higher than the diameter of the B-DNA helix, which shows that the DNA conformation is not completely linear and parallel to the surfactant monolayer. Similar behavior has been observed for the adsorption of large-molecular-weight polylectrolytes on oppositely charged surfaces.[43] Furthermore, the adsorption of DTAB at the same concentration and in the absence of DNA amounts to ∼0.5 mg/m^2 on this type of surface,[23] which clearly indicates that the

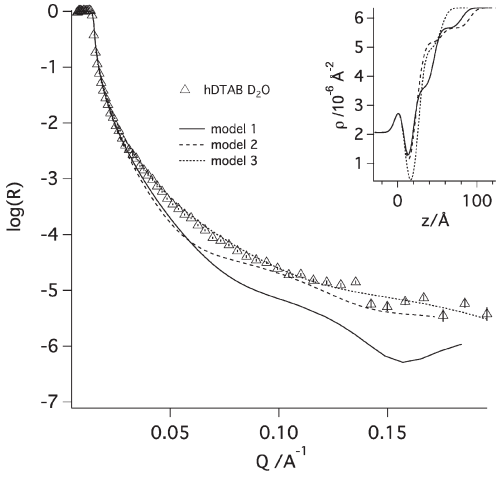

Figure 3. Simulated neutron reflectivity profiles for three different models for the adsorption of DNA and hDTAB to a hydrophobic silica surface in D_2O in which (1) DNA is in direct contact with the surface and DTAB micelles are adsorbed onto its surface, (2) a monolayer of DTAB is in direct contact with the surface and DNA is attached to this layer, or (3) DNA is sandwiched in between a monolayer of DTAB and a layer of DTAB micelles facing the bulk solution. The corresponding data (△) are reproduced from Figure 2.

Table 3. Fitted Parameters (d, ϕ, and δ) Used in the Fits Shown in Figures 2−6[a]

system		d/Å	ϕ/%v/v	δ/Å	A_a/Å^2	Γ/mg m^{-2}	surfactant/DNA base[c]
DTAB-cmc/15-HFOB	DTAB monolayer	9 ± 1	9 ± 1	6 ± 1	50 ± 8	1.0 ± 0.2	0.7
	DNA layer	26 ± 2	38 ± 5	7 ± 3	73 ± 11	1.5 ± 0.2	
DTAB-cmc/150-HFOB	DTAB monolayer	10 ± 5	95 ± 5	4 ± 2	825 ± 354	0.06 ± 0.01	0.3
	DNA layer	45 ± 10	95 ± 5	5 ± 2	523 ± 230	0.21 ± 0.07	
CTAB-cmc/150-HFOB	CTAB monolayer	9 ± 1	10 ± 1	3 ± 1	65 ± 6	0.9 ± 0.1	1.4
	DNA layer	22 ± 2	70 ± 7	3 ± 1	178 ± 46	0.6 ± 0.1	
DTAB-cmc/15-HPHIL	DTAB bilayer	28 ± 2	51 ± 5	3 ± 2	60 ± 6	1.7 ± 0.2	1.3
	DNA layer	42 ± 3	65 ± 7	4 ± 3	80 ± 8	1.3 ± 0.3	

[a] The inner roughness of the Si blocks was as low as 3 ± 1 Å. For C, the inner roughness of the Si blocks was as low as 4 ± 1 Å. There was a natural SiO_2 layer of typically 13 ± 3 Å with 15 ± 5% solvent and a hydrophobic layer of typically 10 ± 1 Å with 25 ± 5% solvent content and a roughness of 6 Å. (See the fits shown in Figure 2.) The area per monomer (A_a) and adsorbed amount (Γ) calculated from the box fits are accurate only when there is no or little interfacial roughness, and thus these values should be taken as guidelines only. [b] Monomer refers to a single surfactant molecule or DNA base pair. [c] Surfactant/base refers to the surfactant/base ratio at the interface between the cationic surfactant layer and the DNA layer.

dx.doi.org/10.1021/la202087u |*Langmuir* 2011, 27, 12506–12514

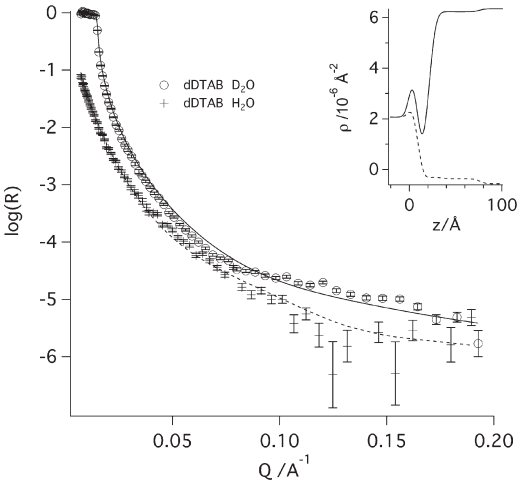

Figure 4. DTAB-cmc/150-HPHOB. Neutron reflectivity profiles for 0.061 mM negative charges of DNA (0.02 mg/mL) and 0.073 mM DTAB on a hydrophobic silica surface. Symbols and lines as described in Figure 2. The inset gives the scattering length density profiles obtained for the best fits (—) given in the main panel.

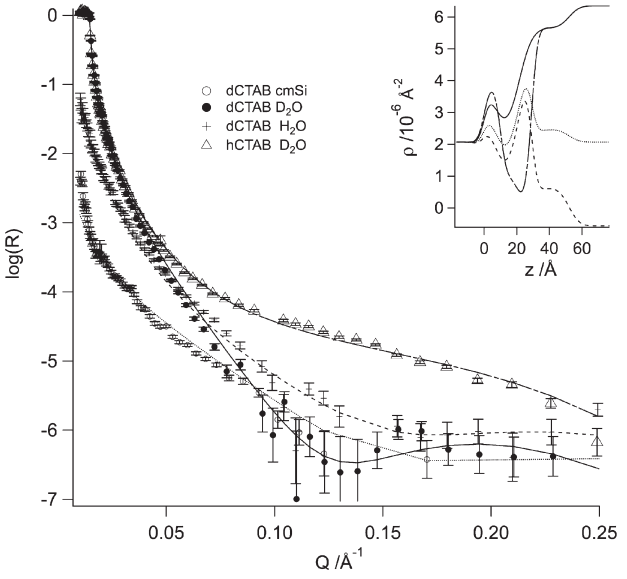

Figure 5. CTAB-cmc/150-HPHOB. Neutron reflectivity profiles for 0.061 mM negative charges of DNA (0.02 mg/mL DNA) and 0.001 mM CTAB mixtures on a hydrophobic silica surface. Symbols and lines are the same as described in Figure 2. The inset gives the scattering length density profiles obtained for the best fits (—) given in the main panel.

DTAB surface coverage is enhanced by the presence of DNA (~1 mg/m^2, Table 3).

Effect of Bulk Concentration: DTAB−DNA on a Hydrophobic Surface at $^1/_{150}$th of the cmc (DTAB-cmc/150-HPHOB). To understand the effect of a lowered DNA/surfactant concentration on the structure of the mixed adsorbed layer explored in DTAB-cmc/15-HPHOB, we performed experiments using 0.02 mg/mL DNA (0.061 mM negative charges) and 0.070 mM DTAB on hydrophobic surfaces. Neutron reflectivity profiles of DNA−DTAB mixtures on hydrophobic surfaces under these conditions are shown in Figure 4 along with the corresponding best fits to the measured data. Table 3 gives the

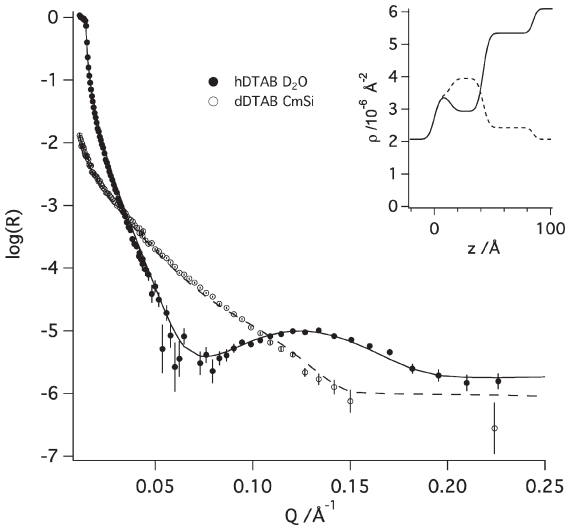

Figure 6. DTAB-cmc/15-HPHIL. Neutron reflectivity profiles for 0.182 mM negative charges of DNA (0.06 mg/mL) and 0.7 mM DTAB mixtures on hydrophilic silica surfaces. Two different isotopic contrasts were used where the symbols and lines correspond to data and fits, respectively: fully deuterated surfactant in cmSi (○, ---) and fully hydrogenated surfactant in D_2O (●, —). The inset gives the scattering length density profiles obtained for the best fits given in the main panel.

parameters used in the fits. In this case, the model that best fits the data is still number 2, in which a thin surfactant layer is in direct contact with the underlying surface and a DNA layer facing the bulk solution. For this low surfactant concentration (in relation to its cmc), there is very little adsorption of both the surfactant (~10 ± 5 Å layer with 95 v/v % solvent) and DNA (~45 ± 10 Å layer with 95 v/v %) compared with that at higher concentrations. The low coverage lowers the thickness sensitivity of NR; nevertheless, the presence of these very diffuse layers is clearly detectable. The results suggest that the presence of DNA at the interface is related to its electrostatic attractive interaction with the adsorbed cationic surfactant and that the amounts of both components at the interface are limited by the surface coverage of surfactant, with the latter being determined by its bulk concentration in relation to its cmc. Indeed, at this DTAB concentration and in the absence of DNA, insignificant adsorption occurs on this type of surface.[23] Although the fitted DNA layer thickness of 45 Å is twice the diameter of B-DNA, a double DNA layer is not likely to occur given the expected high electrostatic repulsion under the low ionic conditions used in this work.

Effect of Surfactant Chain Length: CTAB−DNA on a Hydrophobic Surface at $^1/_{150}$th of the cmc (CTAB-cmc/150-HPHOB). Neutron reflectivity profiles of 0.02 mg/mL DNA (0.061 mM negative charges) and 0.001 mM CTAB on hydrophobic surfaces are shown in Figure 5 along with the corresponding best fits to the measured data. Table 3 gives the parameters used in the fits to model 2 (as in Figure 3) on hydrophobic surfaces, as schematically presented in Figure 8. The observed layer thickness for CTAB is 9 ± 2 Å with 10% solvent by volume just as for the DTAB system. A full CTAB monolayer at the air−water interface gives an area per molecule of ~44 Å and a layer thickness of 16−20 Å.[44] Thus, the monolayer area coverage on the hydrophobic surface is ~45% of a full monolayer. This indicates that the cationic surfactant

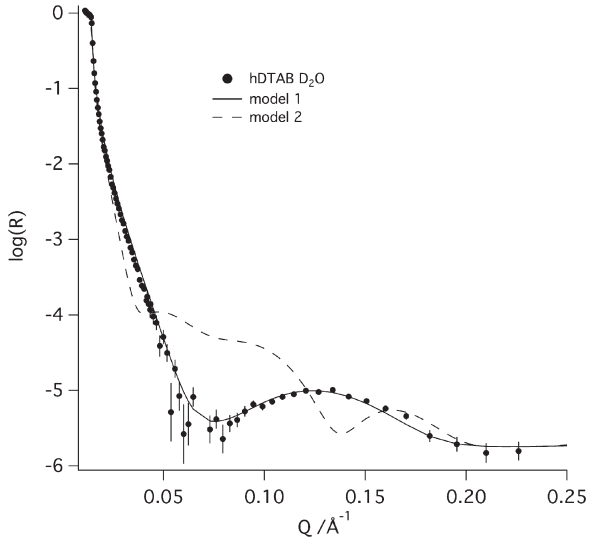

Figure 7. Simulated neutron reflectivity profiles for two different models for the adsorption of DNA and h-DTAB to a hydrophilic silica surface in which (1) a DTAB bilayer is in direct contact with the surface and DNA is attached to this layer or (2) DNA is sandwiched in between two DTAB bilayers, where the outer surfactant layer is less dense. The corresponding data (●) are reproduced from Figure 6.

partially interpenetrates the hydrophobic layer, which is likely given its high porosity. (The Me_2OdCS layer contains 25 v/v % solvent; see Figure 1.) By comparing the results with different surfactant chain lengths (DTAB-cmc/150-HPHOB and CTAB-cmc/150-HPHOB) and the same concentration ratio with respect to the cmc, we can see that the monolayer coverage of surfactant is significantly higher for the CTAB case. This result indicates that the apparent cac at the interface is much lower for DNA/CTAB than for DNA/DTAB adsorption layers, in agreement with observations made by ellipsometry by Cárdenas et al.[23] We have previously demonstrated that the same adsorption in terms of mass on hydrophobic surfaces is observed regardless of the order in which the surface is exposed to DNA and CTAB,[18] and thus the findings presented here cannot be regarded as being affected by the minimal amount of DNA that might be preadsorbed onto the hydrophobic silica surface for the CTAB-cmc/150-HPHOB system. Given that a significantly lower bulk concentration of CTAB ($^1/_{150}$th of the cmc) compared to that for DTAB ($^1/_{15}$th of the cmc) is needed to obtain similar mixed DNA/surfactant interfacial structures, this suggests that CTAB monolayer formation with DNA seems to be a more synergistic process. In fact, for $^1/_{150}$th of the cmc, the surface concentrations of DTAB in the absence (<0.2 mg/m^2)[23] and presence (0.06 mg/m^2, Table 3) of DNA are comparable, but that is not the case for CTAB, in which minimal adsorption in the absence of DNA (<0.2 mg/m^2)[23] occurs while around 0.9 mg/m^2 is found in the presence of DNA (Table 3). The diameter of the B-DNA helix is 21 Å,[42] in good agreement with the fitted layer thickness of 22 ± 2, and the volume fraction of water in the DNA layer (70 ± 5%) indicates a lower coverage than in the DTAB case.

Effect of Surface Properties: DTAB−DNA on a Hydrophilic Surface at $^1/_{15}$th of the cmc (DTAB-cmc/150-HPHIL). Neutron reflectivity profiles for 0.06 mg/mL DNA (or 0.182 mM negative charges) and 0.7 mM DTAB on hydrophilic surfaces are shown in Figure 6 with the corresponding best fits to the measured data. Table 3 gives the parameters used in the fits. Given that DNA

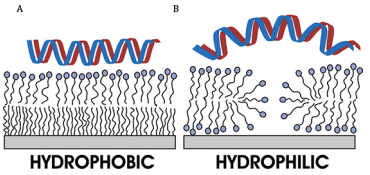

Figure 8. Schematic representation of (A) the mixed DNA−DTAB layer on a hydrophobic substrate where a monolayer of surfactant is directly adsorbed on the hydrophobic surface and DNA molecules in turn are attached to the surfactant layer and (B) the mixed DNA−DTAB layer on a hydrophilic substrate where DTAB admicelles are in direct contact with the surface and to which a less dense layer of DNA is attached.

does not interact directly with hydrophilic silica surfaces,[13] we could imagine two different situations for the mixed DNA−surfactant layer. In model 1, adsorbed DTAB micelles or a bilayer are in direct contact with the hydrophilic substrate and DNA is on top of this layer. In model 2, a second DTAB layer is on top of the DNA facing the bulk solution. Simulated reflectivity profiles for these models are given in Figure 7 for h-DTAB in D_2O. The simulation that clearly best fits the data corresponds to model 1, where DNA molecules are located on top of a DTAB layer that has a thickness corresponding to a micellelike layer or a bilayer. Excellent fits using model 1 are obtained for both contrasts measured (Figure 6), further validating the structure, which is schematically represented in Figure 8. The radius of DTAB micelles in solution has been reported to be 18 Å with a headgroup area of about 81 Å^2 under conditions similar to the ones used in this work.[45] The best fit gives the thickness of the adsorbed surfactant layer to be 28 ± 1 Å. This thickness is in accordance with a DTAB bilayer or flattened adsorbed micelles, which tend to have a slightly lower thickness than the diameter of the micelles in solution.[45,46] The diameter of B-DNA is 21 Å, and the layer thickness obtained in the fit is 42 ± 2 Å, which indicates that the DNA is not lying flat at the interface. Finally, at this surfactant concentration and in the absence of DNA, there is no significant surfactant adsorption on hydrophilic surfaces.

On the Implications of the Proposed Interfacial Structure. On hydrophobic surfaces, a detailed analysis of the charge ratios within the different layers in model 2 (Table 3) can be obtained using the volume fractions of the two fitted layers (cationic surfactant and DNA), the layer thickness, and the molecular volume of each species involved within each layer as shown schematically in Figure 8. To make a proper comparison, we calculate the charge ratio at the interface between the surfactant molecules and the DNA. For that, we must take into account that within the area occupied by each DNA base pair and given its helical nature there are two negative charges, one facing the bulk and another facing the surfactant layer, whereas in the area occupied by a surfactant molecule there is one cationic charge in the hydrophobic surface case and two charges in the hydrophilic surface case. Thus, the positive to negative interfacial charge ratios are ∼0.7 and ∼1.4 for DTAB at cmc/15 and CTAB at cmc/150 on hydrophobic surfaces, respectively. From this, it follows that there are excess cationic charges for CTAB. In this calculation, we have neglected the contribution from the surface charge of the underlying silica surface because it is 2 orders of magnitude lower than these values.[47] The DNA layer contains a larger volume fraction of water than the surfactant layer, probably

as a result of the lateral repulsion between uncompensated for negative charges on the DNA molecules in the interfacial layer, which is a feature observed previously for polyelectrolytes.[43]

We rationalize that the structural model determined with DNA molecules on top of a surfactant monolayer is the most energetically favorable interfacial layer structure given that the hydrophobic alkyl chains of the surfactant molecules are facing the hydrophobic substrate, thus minimizing the entropic cost of arranging water molecules around the hydrophobic moieties. The alignment of the DNA molecule parallel to the surfactant monolayer maximizes the attractive electrostatic interaction between the negatively charged DNA backbone and the positively charged surfactants, which leads to the release of counterions maximizing the entropy of the system. Compensating for the excess negative charge would require the adsorption of another ~0.62 surfactant per base pair. The absence of surfactant on top of the DNA layer indicates that compensation for the excess surface charge by Na^+ counterions is more favorable than the adsorption of more surfactant, which would leave its alkyl chains exposed to the aqueous subphase because the surfactant concentration is not sufficient to form micellar aggregates on top of the DNA layer. This is consistent with the DNA presenting a hydrophilic surface on which the formation of a surfactant monolayer with the hydrophobic chains facing the solution is unfavorable. A bilayer or micelle layer could potentially form on top of the DNA layer and face the bulk solution. However, the surface cac of a surfactant at hydrophilic surfaces is typically on the order of 0.6−0.85 of the bulk cmc of the surfactant,[21] and thus we would not expect surfactant adsorption on the DNA under the bulk conditions used: the cmc of CTAB is 0.15 mM, and that of DTAB is 11 mM. Nevertheless, we cannot rule out that there is a very dilute layer of surfactant micelles on top of the DNA because of the poor contrasting conditions (the NR profiles are not sensitive to an additional layer with 0−5 v/v % surfactant), but in any case, this low coverage would not be sufficient to neutralize the excess negative charge of the system. We cannot rule out a small penetration of surfactant within the DNA layer either.

A recent NR report on the interaction between short fragments of DNA (similar to its persistence length) and DTAB at the air−water interface showed that no adsorption of DNA−DTAB complexes at the interface occurs at bulk charge ratios similar to those used in this work.[20] At lower charge ratios, though, DNA was located below a surfactant monolayer at the air−water interface, and there was an additional diffuse layer of surfactant micelles under the DNA, facing the bulk. From the volume fractions reported and the layer thicknesses given in their work, the authors report an excess of 76 positive to negative charges within the adsorbed layer for 1.7 mM DTAB. However, if longer DNA chains (several kDa) were used, then DNA formed a very diffuse layer under the cationic surface. The net DNA concentration used by Kundu et al.[20] was considerably higher than those used in this work (0.33 mg/mL as compared to 0.06−0.02 mg/mL), and differences in the cac's could be expected in different publications as evidenced by the phase diagram for DNA−DTAB.[28] Earlier experiments on hydrophobic surfaces performed in our group have found no major differences in the interfacial behavior of long and short DNA molecules in the presence of surfactants.[18] Similarly, Zhang et al.[19] found that DNA coadsorbed at the air−water interface in the presence of at least 0.1 mM DTAB. In this case, the net DNA concentration was 1 order of magnitude lower than those used in this work, and thus no direct comparisons with our results can be drawn given the large differences in the required surfactant concentration to induce phase separation. Nevertheless, DNA coadsorption is seen in all cases (as in our work), and several DNA−CTAB layers were observed at the interface only when a great excess of cationic charges was present in the system.

A direct comparison of the charge ratio densities between DTAB-cmc/15-HPHOB and HPHIL is not physically helpful, even though the same bulk DTAB concentration was used, because the conformations of the DNA and surfactant layer differ depending on the type of underlying surface: the surface charge ratio at the interface between DNA and DTAB would indicate excess positive charges on the hydrophilic surface, and there is no overcompensation on the hydrophobic surface (Table 3). In reality, the amount of DNA is the same in both cases, but the area occupied by each surfactant is smaller on hydrophobic than on hydrophilic surfaces. Thus, it seems that the limiting factor for DNA compaction at interfaces is the surface concentration of surfactant rather than the type of surface.

We rationalize that the structure, with DNA molecules located on top of a DTAB bilayer (or a layer of flattened micelles/islands), is the most energetically favorable interfacial structure given that the electrostatic interaction between the positively charged surfactant molecules and both the negatively charged surface and DNA molecules increases the entropy of the system by the release of the maximum number of counterions. As in the case of the hydrophobic surfaces, the lack of surfactant on top of the DNA is consistent with the low bulk surfactant concentration, which is far below its surface cac, but we cannot rule out the presence of a very dilute layer (up to 5 v/v %) of surfactant micelles on top of the DNA or individual surfactant molecules within the DNA layer.

The structures of DNA−CTAB and DNA−DTAB aggregates differ in the bulk.[48] A hexagonal phase is found for DNA−CTAB in which the CTAB cylindrical micelles have a distorted structure to maximize the electrostatic interactions with DNA whereas a cubic disordered structure is found for DNA−DTAB, also to maximize the electrostatic interactions. Our NR experiments indicate clear differences in the packing of DNA at the surfaces in terms of its conformation (either it sits nearly parallel to the interface or allows for a certain flexibility in the direction perpendicular to the interface) that are related to the surfactant and the solution concentration rather than the underlying surface properties or the structure of the phases formed upon phase separation. It is clear that the amount of surfactant adsorbing on the surface (regardless of its nature) seems to be the critical parameter in determining how much DNA is bound to the surface and which conformation it has. On the basis of these results, we can speculate that using a higher ionic strength could lead to an increased amount of DNA compacted on the surfaces. Finally, we note that the surface excesses calculated from our fits to the NR data (Table 3) are very consistent with those observed by ellipsometry, which further supports the optical models chosen to fit the NR data.[23]

CONCLUSIONS

Neutron reflectometry was successfully used to determine the structure of mixed DNA−cationic surfactant layers at hydrophilic and hydrophobic silica surfaces. The H/D contrast variation technique was essential to elucidating the interfacial structures. Regardless of the surface properties, we found that

in the interfacial complexes of DNA and DTAB/CTAB the DNA molecules are located on top of a self-assembled surfactant layer, with the thickness of the DNA layer and the surfactant−DNA ratio determined by the surface coverage of the underlying cationic layer. The amount of DNA coadsorbed with a cationic surfactant depends largely on the surface coverage of surfactant, which itself is determined by the type of surface (hydrophobic > hydrophilic surface), the bulk surfactant concentration with respect to its cmc (high versus low), and the hydrophobicity of the surfactant (CTAB > DTAB). The DNA coverage is generally lower than that of the surfactant, perhaps because of electrostatic repulsion due to uncompensated DNA negative charges. When the surfactant coverage is high, the DNA is orientated parallel to the interface, but at lower surfactant coverages, DNA adopts a more flexible conformation at the interface, thus demonstrating that the amount and conformation of DNA at the interface can be tuned according to the experimental conditions employed. Our findings suggest that manipulating the charge and stability of the nanocarriers and nanocolloids could enhance the efficiency of DNA packing and transport across the cell membrane.

AUTHOR INFORMATION

Corresponding Author

*Fax: +4535325217. Tel: +4535320469. E-mail: cardenas@nano.ku.dk.

REFERENCES

(1) Trewavas, A. *Anal. Biochem.* **1967**, *21*, 324–239.
(2) Del Sal, G.; Manfioletti, G.; Schneider, C. *Biotechniques* **1989**, *7*, 514–520.
(3) Verma, I. M.; Somia, N. *Nature* **1997**, *389*, 239–242.
(4) Templeton, N. S.; Lasic, D. D. *Mol. Biotechnol.* **1999**, *11*, 175–180.
(5) Piculell, L.; Lindman, B.; Karlström, G. Phase Behavior of Polymer Surfactant Systems. In *Polymer-Surfactant Systems*; Kwak, J. C. T., Ed.; Marcel Dekker: New York, 1998; pp 65−141.
(6) Nylander, T.; Samoshina, Y.; Lindman, B. *Adv. Colloid Interface Sci.* **2006**, *123−126*, 105–123.
(7) Mel'nikov, S. M.; Segeryev, V. G.; Yoshikawa, K. *J. Am. Chem. Soc.* **1995**, *117*, 2401–2408.
(8) Mel'nikov, S. M.; Sergeyev, V. G.; Yoshikawa, K. *J. Am. Chem. Soc.* **1995**, *117*, 9951–9956.
(9) Dias, R.; Innerlohinger, J.; Glatter, O.; Miguel, M.; Lindman, B. *J. Phys. Chem. B* **2005**, *109*, 10458–10463.
(10) Ainelem, M. L.; Nylander, T. *Soft Matter* **2011**, *7*, 4577–4594.
(11) Koltover, I.; Salditt, T.; Rädler, J. O.; Safinya, C. R. *Science* **1998**, *281*, 78–81.
(12) Rädler, J. O.; Koltover, I.; Salditt, T.; Safinya, C. R. *Science* **1997**, *275*, 810–814.
(13) Zantl, R.; Baicu, L.; Artzner, F.; Sprenger, I.; Rapp, G.; Rädler, J. O. *J. Phys. Chem. B* **1999**, *103*, 10300–10310.
(14) Guillot, S.; McLoughlin, D.; Jain, N.; Delsanti, M.; Langevin, D. *J. Phys.: Condens. Matter* **2003**, *15*, S219–S224.
(15) Leal, C.; Wadsö, L.; Olofsson, G.; Miguel, M.; Wennerström, H. *J. Phys. Chem. B* **2004**, *108*, 3044–3050.
(16) Braem, A. D.; Prieve, D. C.; Tilton, R. D. *Langmuir* **2001**, *17*, 883–890.
(17) Dèdinaité, A.; Claesson, P. M.; Bergström, M. *Langmuir* **2000**, *16*, 5257–5266.
(18) Cárdenas, M.; Braem, A.; Nylander, T.; Lindman, B. *Langmuir* **2003**, *19*, 7712–7718.
(19) Zhang, J.; Taylor, D. J. F.; Li, P. X.; Thomas, R. K.; Wang, J. B. *Langmuir* **2008**, *24*, 1863–1872.
(20) Kundu, S.; Langevin, D.; Lee, L. T. *Langmuir* **2008**, *24*, 12347–12353.
(21) Cárdenas, M.; Campos-Téran, J.; Nylander, T.; Lindman, B. *Langmuir* **2004**, *20*, 8597–8603.
(22) Cárdenas, M.; Nylander, T.; Dreiss, C.; Cosgrove, T.; Lindman, B. *Langmuir* **2005**, *21*, 3578–3583.
(23) Cárdenas, M.; Nylander, T.; Thomas, R. K.; Lindman, B. *Langmuir* **2005**, *21*, 6495–6502.
(24) Cárdenas, M.; Schillén, K.; Nylander, T.; Jansson, J.; Lindman, B. *Phys. Chem. Chem. Phys.* **2004**, *6*, 1603–1607.
(25) Cárdenas, M.; Schillén, K.; Pebalk, D.; Nylander, T.; Lindman, B. *Biomacromolecules* **2005**, *6*, 832–837.
(26) Atkin, R.; Craig, V. S. J.; Wanless, E. J.; Biggs, S. *Adv. Colloid Interface Sci.* **2003**, *103*, 219–304.
(27) Stubenrauch, C.; Albouy, P.-A.; v. Klizing, R.; Langevin, D. *Langmuir* **2000**, *16*, 3206–3213.
(28) Dias, R.; Mel'nikov, S.; Lindman, B.; Miguel, M. G. *Langmuir* **2000**, *16*, 9577–9583.
(29) Eskilsson, K.; Leal, C.; Lindman, B.; Miguel, M.; Nylander, T. *Langmuir* **2001**, *17*, 1666–1669.
(30) Fragneto-Cusani, G. *J. Phys.: Condens. Matter* **2001**, *13*, 4973–4989.
(31) Nylander, T.; Campbell, R. A.; Vandoolaeghe, P.; Cardenas, M.; Linse, P.; Rennie, A. R. *Biointerfaces* **2009**, *3*, FB64–FB82.
(32) Lu, J. R.; Thomas, R. K. *J. Chem. Soc., Faraday Trans.* **1998**, *94*, 995–1018.
(33) Thomas, R. K. *Annu. Rev. Phys. Chem.* **2004**, *55*, 391–426.
(34) Campbell, R. A.; Wacklin, H.; Sutton, I.; Cubitt, R.; Fragneto, G. *Eur. Phys. J. Plus* **2011**submitted for publication.
(35) Cubitt, R.; Fragneto, G. *Appl. Phys. A: Mater. Sci. Process.* **2002**, *74*, S329–S331.
(36) Vandoolaeghe, P.; Rennie, A. R.; Campbell, R. A.; Nylander, T. *Langmuir* **2009**, *25*, 4009–4020.
(37) Doshi, D. A.; Watkins, E. B.; Israelachvili, J. N.; Majewski, J. *Proc. Nat. Acad. Sci. U.S.A.* **2005**, *102*, 9458–9462.
(38) Majkrzak, C. F.; Satija, S. K.; Berk, N. F.; Borchers, J. A.; Dura, J. A.; Ivkov, R.; O'Donovan, K. *Neutron News* **2001**, 25–29.
(39) Nelson, A. *J. Appl. Crystallogr.* **2006**, *39*, 273–276.
(40) Abeles, F. *Ann. Phys.* **1948**, *3*, 504–520.
(41) Lyttle, D. J.; Lu, J. R.; Su, T. J.; Thomas, R. K.; Penfold, J. *Langmuir* **1996**, *11*, 1001–1008.
(42) Cantor, C. R.; Schimmel, P. R. *Biophysical Chemistry*; W. H. Freeman & Co: San Francisco, 1980; p 1371.
(43) Samoshina, Y.; Nylander, T.; V., S.; Bauer, R.; Eskilsson, K. *Langmuir* **2005**, *21*, 5872–5881.
(44) Lu, J. R.; Hromadova, E.; Simister, A.; Thomas, R. K.; Penfold, J. *J. Phys. Chem.* **1994**, *98*, 11519–11526.
(45) Imae, T.; Ikeda, S. *J. Phys. Chem.* **1986**, *90*, 5216–5223.
(46) Fragneto, G. *Langmuir* **1996**, *12*, 6036–6043.
(47) Iler, R. K. *The Chemistry of Silica: Solubility, Polymerization, Colloid and Surface Properties, and Biochemistry*; Wiley: New York, 1979; p 866.
(48) Lindman, B. Dias, R. In *DNA Interactions with Polymers and Surfactants*; Dias, R., Lindman, B., Eds.; Wiley-Interscience: Hoboken, NJ, 2008.
(49) Jacrot, B. *Rep. Prog. Phys.* **1976**, *39*, 911–953.
(50) Weast, R. C., Ed. *Handbook of Chemistry and Physics*, 54th ed.; Chemical Rubber Company: Cleveland, OH, 1973.